

# A 6G Oriented High-Throughput Satellite Communication Demodulation Method

Zhijie Mao\*

School of Information  
Communication, National University  
of Defense Technology, Xi'an Shannxi  
China,  
2657262006@qq.com

Guangen Wu

School of Information  
Communication, National University  
of Defense Technology, Xi'an Shannxi  
China,  
584051352@163.com

Lin Zhou

School of Information  
Communication, National University  
of Defense Technology, Xi'an Shannxi  
China,  
zhou8201@163.com

## ABSTRACT

The integration of satellite communication system and 6G wireless system forms an ubiquitous and real global communication system, and the satellite communication capacity and data throughput will increase rapidly. A 6G oriented high-throughput satellite communication modulation and demodulation method is proposed. The method is not only suitable for MAPSK modulation and demodulation in nonlinear networks, moreover, the reliability and throughput of information transmission are improved. And the effectiveness of this method is verified by computer simulation.

## CCS CONCEPTS

• **Human-centered computing**; • **Human computer interaction (HCI)**; • **Interaction paradigms**;

## KEYWORDS

High throughput satellite, 6G wireless communication, MAPSK, Bit error ratio (BER)

### ACM Reference Format:

Zhijie Mao\*, Guangen Wu, and Lin Zhou. 2021. A 6G Oriented High-Throughput Satellite Communication Demodulation Method. In *The 5th International Conference on Computer Science and Application Engineering (CSAE 2021), October 19–21, 2021, Sanya, China*. ACM, New York, NY, USA, 5 pages. <https://doi.org/10.1145/3487075.3487140>

## 1 INTRODUCTION

The distance between the orbiting satellite in the satellite communication system and the ground terminal is generally thousands to tens of thousands of kilometers, most of which are in vacuum space. The atmosphere about 50km thick from the ground and the ionosphere about 1000km thick above the atmosphere. There is not only a sudden change dielectric layer between outer space and ionosphere, but also between ionosphere and atmosphere. Although they are the same medium, the density of medium distribution varies with the height, and the medium distribution is not nonlinear.

Permission to make digital or hard copies of all or part of this work for personal or classroom use is granted without fee provided that copies are not made or distributed for profit or commercial advantage and that copies bear this notice and the full citation on the first page. Copyrights for components of this work owned by others than ACM must be honored. Abstracting with credit is permitted. To copy otherwise, or republish, to post on servers or to redistribute to lists, requires prior specific permission and/or a fee. Request permissions from [permissions@acm.org](mailto:permissions@acm.org).

CSAE 2021, October 19–21, 2021, Sanya, China  
© 2021 Association for Computing Machinery.  
ACM ISBN 978-1-4503-8985-3/21/10...\$15.00  
<https://doi.org/10.1145/3487075.3487140>

In addition, the satellite is far away in space, which greatly limits the transceiver power of the satellite. Therefore, when satellites and ground terminals communicate with each other, the transmission channel carrying information is a very complex nonlinear medium, and the power of transceiver equipment is greatly limited. The baseband modulation method only applied to land surface spatial linear transmission medium is not suitable for nonlinear channel [1, 2].

To extend a wider application scenario, combining the satellite communication system with the 6G mobile communication system [3-5] forms a ubiquitous and real global communication system. The satellite communication capacity and data throughput will increase rapidly, and the traditional baseband modulation QPSK has lost its application value. The traffic of traditional satellite communication is not large enough, higher-order APSK modulation and demodulation is not required, and the reliability of transmission information is high. Moreover, the cost of higher-order APSK modulation and demodulation technology is higher because of the complexity of satellite communication channel. When the future mobile communication system integrates the satellite communication system, compared with the traditional satellite communication standards, the relevant technical standards of information traffic and data transmission reliability will change greatly, or even completely the opposite. It is certain that in the baseband modulation and demodulation technology integrated into 6G satellite communication system, there must be higher-order APSK.

This paper proposes a high-order APSK soft modulation and demodulation communication model for 6G high-throughput satellite firstly. Based on the modulation/demodulation of QAM and 16APSK signal, this paper focuses on the soft demodulation methods of 64APSK, and then gives the analytical relationship between the upper bound of BER and the influence factor. Finally, the performance simulation and conclusion of the system are given.

## 2 MAPSK DEMODULATION MODEL FOR 6G HIGH THROUGHPUT SATELLITE

In order to meet the requirements of high-throughput satellite information transmission, a MAPSK modulation and demodulation communication process flow model for 6G high-throughput satellite is designed, as shown in Figure 1. Among them, high-order APSK soft modulation/demodulation is adopted for baseband signal. LDPC/Polar coding technology based on 6G is adopted for channel codec. QC-LDPC coding is adopted in simulation experiment, and the check matrix is  $8 \times 16$  order orthogonal sparse matrix,

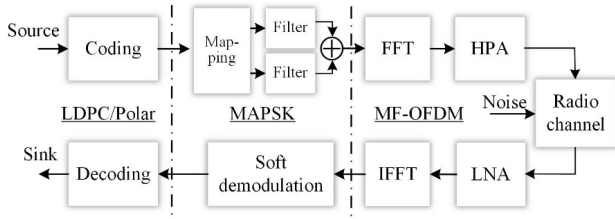


**Figure 1: MAPSK Modulation/Demodulation Communication Model for 6G High Throughput Satellite.**

code length 9216, check matrix is divided into 8 regions, each region is  $4 \times 4$ . Multiple access addressing adopts 6G multifrequency MF-OFDM, which is filtered and transmitted through power amplification (HPA). To realize the convenience of information processing, MAPSK modem and QC-LDPC coded check matrix  $H$ , subcarrier mapping and FFT (IFFT) of FM-OFDM multiple access technology are independent processing systems. Therefore, the dimension number of matrix  $H$  and the order of baseband modulation do not intersect with the sampling number in Fourier transform, as shown in the figure. For the modem in the simulation model, it can adapt to APSK of any order.

QAM is a two-dimensional modulation and demodulation technology with amplitude and phase modulation for 5G. MAPSK is mainly phase modulation, supplemented by amplitude modulation. The modulation order of phase and amplitude can be adjusted at the same time. However, the constellation composed of MAPSK modulation symbols is distributed on multi-layer circles with amplitude as radius. The amplitude fluctuation of the modulation signal is relatively small, and high spectral efficiency can still be obtained. More importantly, the modulation order of amplitude and phase of MAPSK can be changed at the same time, the system appropriately adjusts the proportion of amplitude and phase modulation order with the needs of practical application, so that it can obtain the best modulation effect, rather than QAM can only select the modulation order of square constellation, which limits the arbitrary selection of modulation order.

LDPC coding and MAPSK modulation are combined in the communication system in DVD-S2X standard protocols [6, 7]. The input and output of LDPC Encoding and decoding algorithm are soft information. The communication system needs soft input and soft output operations. Therefore, the output of MAPSK demodulation algorithm is no longer the hard decision information of 0,1, but the soft information of probability likelihood ratio, that is, soft demodulation output. This greatly increases the computational complexity of the whole space-time communication system. To reduce the computational complexity and reduce the storage capacity, it is particularly important to realize the research of MAPSK soft demodulation algorithm.

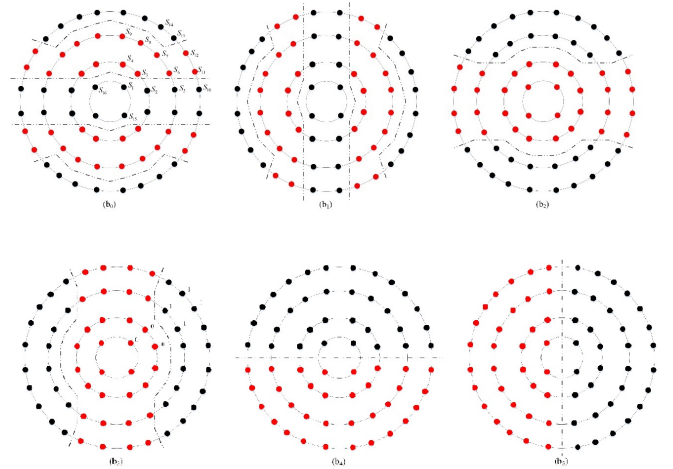


**Figure 2: 64APSK(4+12+20+28) of b0,b1,b2,b3,b4,and b5 Binary Coding.**

### 3 MAPSK SOFT DEMODULATION METHOD BASED ON AMPLITUDE PHASE JOINT MAPPING

For the convenience of description, taking 64APSK signal as an example, a 6G joint MAPSK soft demodulation algorithm is designed and proposed. This method is used in combination with LDPC/Polar encoding and decoding. The soft information output by the demodulator is sent to the decoder, and the digital symbol 0 or 1. It is hard determined bit by bit in the decoder. For the 64APSK(4+12+20+28-APSK) constellation recommended in CCSDS131.2[6,7], as shown in Figure 2, there are four different radii of inner and outer circles. Let the radius of circle be  $R_1, R_2, R_3, R_4$ , which meets  $R_1 < R_2 < R_3 < R_4$ . As shown in Figure 2, 64APSK modulation signal expression is as follows:

$$\begin{aligned} S_k(t) &= \text{Re} \{ I(t) + jQ(t)e^{jw_c t} \} \\ &= I_k(t)\cos(w_c t) + Q_k(t)\sin(w_c t) \\ &= A_I g(t)\cos(w_c t) + A_Q g(t)\sin(w_c t) \end{aligned} \quad (1)$$

where  $S_k(t)$  represents the modulated signal,  $w_c$  represents the frequency of the carrier,  $I_k(t), Q_k(t)$  represents the in-phase and quadrature component of the modulated signal,  $A_I$  represents the amplitude information  $I_k(t)$  of the in-phase component of the modulated signal,  $A_Q$  represents the amplitude information  $Q_k(t)$  of the quadrature of the signal, and  $g(t)$  represents the signal pulse transmitted by the transmitter.

The amplitude and phase of the received  $k$  complex value signal are  $R_k = \sqrt{I_k^2(t) + Q_k^2(t)}$ ,  $\phi_k = \tan^{-1}[Q_k(t)/I_k(t)]$ , for each constellation point, there are six binary vectors  $\{b_5, b_4, b_3, b_2, b_1, b_0\}$ . The algorithm first determines which layer of circle the signal by computing the amplitude  $R_k$  of the received signal. And then determines the specific constellation point of the received signal with the phase of the received signal. Once the constellation point of the received signal is determined, the 6-bit vector value can be determined at one time.

(1) For the received 64APSK signal, in Figure 2, as  $R_k < \frac{R_1+R_2}{2}$ , for the lowest bit,  $\{b_{k1}, b_{k0}\} = 1, \{b_{k3}, b_{k2}\} = 0$ . For  $b_{k4}$ , the binary codes of the points above the  $I$  axis are all 1, the points below the  $I$  axis are all 0, and the sinusoids of the phase are all negative in the first quadrant and the second quadrant. Taking the value of the inner circle signal point ( $45^\circ$  and  $135^\circ$ ) as 1, the soft output will be greater than 1 near the vertical axis, and the closer to the horizontal axis, the closer to zero. If the soft output result is greater than zero, the reliability is higher. Similarly, for the two constellation points in the three and four quadrants, the soft output is set to -1. If the soft output result is negative, and the farther away from the zero value, the higher the reliability. Therefore, the lowest soft output on the inner circle can be expressed as  $b_{k4} = -\sin \phi_k / \sin(\pi/4)$ . For  $b_{k5}$ , it is 1 in the first and fourth quadrants and 0 in the second and third quadrants, so the soft output result can be expressed as  $b_{k5} = -\cos \phi_k / \cos(\pi/4)$ . Then there

$$\begin{cases} b_{k0} = b_{k1} = \frac{1}{R_2-R_1} \left( R_k - \frac{R_1+R_2}{2} \right) \\ b_{k2} = b_{k3} = -\frac{1}{R_3-R_2} \left( R_k - \frac{R_2+R_3}{2} \right) \\ b_{k4} = -\sin \phi_k / \sin(\pi/4) \\ b_{k5} = -\cos \phi_k / \cos(\pi/4) \end{cases} \quad (2)$$

(2) As  $\frac{R_1+R_2}{2} \leq R_k < \frac{R_2+R_3}{2}$ , for  $b_{k0}$ , the characteristics of 64APSK constellation, the points of the second, third, fourth, fifth and sixth quadrants and the first quadrant were symmetrical about the coordinate axis and could be folded to the first quadrant. Therefore, the sine and cosine values can be taken as absolute values. If the soft output at  $\pi/12$  is -1 and the soft output at  $\pi/4$  is 1, the bit mapping soft output of the first bit can be obtained through linear transformation, which is  $b_{k0} = \frac{12}{\pi} \text{angle}(|\cos \phi_k| + j|\sin \phi_k|) - 2$ ; Similarly,  $b_{k1} = -\frac{12}{\pi} \text{angle}(|\cos \phi_k| + j|\sin \phi_k|) + 4$ ; For  $\{b_{k3}, b_{k2}\} = 0$ ,  $b_{k2} = b_{k3} = -\frac{1}{R_3-R_2} \cdot (R_k - \frac{R_2+R_3}{2})$ ; For  $\{b_{k5}, b_{k4}\}$ , similar to (1)  $\{b_{k5}, b_{k4}\}$  is defined as follows

$$\begin{cases} b_{k0} = \frac{12}{\pi} \text{angle}(|\cos \phi_k| + j|\sin \phi_k|) - 2 \\ b_{k1} = -\frac{12}{\pi} \text{angle}(|\cos \phi_k| + j|\sin \phi_k|) + 4 \\ b_{k2} = b_{k3} = -\frac{1}{R_3-R_2} \left( R_k - \frac{R_2+R_3}{2} \right) \\ b_{k4} = -\sin \phi_k / \sin(\pi/12) \\ b_{k5} = -\cos \phi_k / \cos(\pi/12) \end{cases} \quad (3)$$

(3) As  $\frac{R_2+R_3}{2} \leq R_k < \frac{R_3+R_4}{2}$ , the design for  $\{b_{k3}, b_{k2}, b_{k1}, b_{k0}\}$  was similar to that in (2)  $\{b_{k1}, b_{k0}\}$ ; For  $\{b_{k5}, b_{k4}\}$  is similar to (1)  $\{b_{k5}, b_{k4}\}$ , that is

$$\begin{cases} b_{k0} = \frac{20}{\pi} \text{angle}(|\cos \phi_k| + j|\sin \phi_k|) - 2 \\ b_{k1} = -\frac{20}{\pi} \text{angle}(|\cos \phi_k| + j|\sin \phi_k|) + 4 \\ b_{k2} = -\frac{20}{\pi} \text{angle}(|\cos \phi_k| + j|\sin \phi_k|) + 4 \\ b_{k3} = \frac{20}{\pi} \text{angle}(|\cos \phi_k| + j|\sin \phi_k|) - 6 \\ b_{k4} = -\sin \phi_k / \sin(\pi/20) \\ b_{k5} = -\cos \phi_k / \cos(\pi/20) \end{cases} \quad (4)$$

(4) As  $R_k > \frac{R_3+R_4}{2}$ , for  $b_{k0}$ , let  $\phi' = \text{angle}(|\cos \phi_k| + j|\sin \phi_k|)$ , if  $\phi' < \frac{3\pi}{28}$ ,  $b_{k0} = -\frac{1}{R_4-R_3} (R_k - \frac{R_3+R_4}{2})$ ;  
if  $\phi' \geq \frac{3\pi}{28}$ ,  $b_{k0} = -\frac{28}{\pi} \text{angle}(|\cos \phi_k| + j|\sin \phi_k|) + 6$ .  
For  $b_{k1}$ , let  $\phi' = \text{angle}(|\cos \phi_k| + j|\sin \phi_k|)$ ,  
if  $\phi' < \frac{9\pi}{28}$ ,  $b_{k1} = -\frac{1}{R_4-R_3} (R_k - \frac{R_3+R_4}{2})$ ;  
if  $\phi' \geq \frac{9\pi}{28}$ ,  $b_{k1} = -\frac{28}{\pi} \text{angle}(|\cos \phi_k| + j|\sin \phi_k|) + 12$ .

For  $\{b_5, b_4, b_3, b_2\}$ , it can be written as follows

$$\begin{cases} b_{k2} = -\frac{28}{\pi} \text{angle}(|\cos \phi_k| + j|\sin \phi_k|) + 4 \\ b_{k3} = \frac{28}{\pi} \text{angle}(|\cos \phi_k| + j|\sin \phi_k|) - 10 \\ b_{k4} = -\sin \phi_k / \sin(\pi/28) \\ b_{k5} = -\cos \phi_k / \cos(\pi/28) \end{cases} \quad (5)$$

#### 4 ANALYTICAL METHOD OF BER UPPER BOUND OF HIGHER-ORDER APSK

Starting from the constellation structure of MAPSK and combined with typical nonlinear channel characteristics, the bit error performance of MAPSK is analyzed. Taking the bit error performance analysis of 64APSK as an example, this method is also suitable for the bit error performance analysis of other MAPSK ( $M=16,32,64,128$ ) in nonlinear channel. MAPSK constellation is the constellation structure recommended in CCSDS131.2 blue book. The 64APSK constellation is composed of four concentric rings. In Figure 2, the variable parameters can be attributed to the radius ratio  $\rho_i$  and the relative rotation difference between the rings. In order to preserve the regularity of 64APSK constellation, the relative rotation between rings is generally not considered, that is, the phase difference is only set to 0. On the 64APSK constellation, the ratio of each ring radius is defined as follows

$$\rho_1=R_2/R_1, \rho_2=R_3/R_1, \rho_3=R_4/R_1 \quad (6)$$

Then the average symbol energy of 64APSK constellation is defined as:

$$E_s = \left( 1 + 3\rho_1^2 + 5\rho_2^2 + 7\rho_3^2 \right) R_1^2 / 16 = \alpha R_1^2 \quad (7)$$

Where the parameter  $\alpha = (1 + 3\rho_1^2 + 5\rho_2^2 + 7\rho_3^2) / 16$  is expressed as a function of the radius ratio.

For M-order modulation, the upper bound of symbol error ratio (SER) can be expressed as

$$P(E) = \frac{1}{M} \sum_{i=1}^M P(E|s_i) \leq \frac{1}{M} \sum_{i=1}^M \sum_{j \neq i}^M p(s_i \rightarrow s_j) \quad (8)$$

where  $P(E)$  it represents the probability of error event, and the probability of  $p(s_i \rightarrow s_j)$  erroneous decision as a symbol  $s_j$  when the transmitted symbol is  $s_i$ . In the case of maximum likelihood detection demodulator, the decision region of each symbol is the relative unit where each symbol is located. Because the points on each ring of MAPSK in CCSDS131.2 are evenly distributed, the probability of error code as adjacent symbols is the same. Therefore, when calculating the upper bound of bit error, only one symbol needs to be taken on each ring to approximate the error probability of other symbols on the ring, as shown in Figure 2. Based on the above assumptions, the SER upper bound of 64APSK can be expressed as the accumulation of probability terms equal to the number of constellation rings, that is

$$P(E)_{64APSK} = \frac{1}{M} \sum_{i=1}^N P(E|s_k) \times \frac{n_i}{M} \quad (9)$$

where  $N$  is the total number of rings on the constellation,  $n_i$  is the total number of symbols on the  $i$  ring, and is the probability of  $P(E|s_k)$  is the  $k$  symbol error. The 64APSK constellation is

composed of four concentric rings, so the SER under the maximum likelihood detector is

$$P(E)_{64APSK} = \frac{1}{16} [P(E|s_1) + 3P(E|s_3) + 5P(E|s_7) + 7P(E|s_{13})] \quad (10)$$

And the corresponding error modess $s_1, s_3, s_7, s_{13}$  can be expressed as follows

$$\begin{cases} P(E|s_1) = \sum_{j=2,3,4,15,16} p(s_1 \rightarrow s_j) \\ P(E|s_3) = \sum_{j=1,2,4,7} p(s_3 \rightarrow s_j) \\ P(E|s_7) = \sum_{j=3,6,8,13} p(s_7 \rightarrow s_j) \\ P(E|s_{13}) = \sum_{j=7,12,14} p(s_{13} \rightarrow s_j) \end{cases} \quad (11)$$

At the same time, the error probability $p(s_i \rightarrow s_j)$ is also expressed as a function of the constellation points Euclidean distance $d_{ij}$ and the noise power density spectrum $N_o$ , that is $p(s_i \rightarrow s_j) = f(d_{ij}/\sqrt{2N_o})$ .Which is substituted into the above formula

$$\begin{aligned} P(E)_{64APSK} \leq & \frac{1}{8} f\left(\frac{d_{1,2}}{\sqrt{2N_o}}\right) + \frac{1}{4} f\left(\frac{d_{1,3}}{\sqrt{2N_o}}\right) + \frac{1}{8} f\left(\frac{d_{1,15}}{\sqrt{2N_o}}\right) \\ & + \frac{3}{8} f\left(\frac{d_{3,2}}{\sqrt{2N_o}}\right) + \frac{1}{2} f\left(\frac{d_{3,7}}{\sqrt{2N_o}}\right) + \frac{5}{8} f\left(\frac{d_{7,6}}{\sqrt{2N_o}}\right) \\ & + \frac{3}{4} f\left(\frac{d_{7,13}}{\sqrt{2N_o}}\right) + \frac{7}{8} f\left(\frac{d_{13,12}}{\sqrt{2N_o}}\right) \end{aligned} \quad (12)$$

The Euclidean distance between constellation points is defined as follows

$$\begin{cases} d_{1,2} = \sqrt{(1 + \rho_1^2 - 2\rho_1 \cos \pi/6)} R_1^2, & d_{1,3} = (\rho_1 - 1) R_1, \\ d_{1,15} = \sqrt{2} R_1, & d_{3,2} = 2\rho_2 R_1 \sin \pi/12, \\ d_{3,7} = (\rho_2 - \rho_1) R_1, & d_{7,6} = 2\rho_2 R_1 \sin \pi/20, \\ d_{7,13} = (\rho_3 - \rho_2) R_1, & d_{13,12} = 2\rho_3 R_1 \sin \pi/28 \end{cases} \quad (13)$$

From the above formula, the SER upper bound of 64APSK is as follows

$$\begin{aligned} P(E)_{64APSK} \leq & \frac{1}{8} f\left(\sqrt{\frac{(1 + \rho_1^2 - 2\rho_1 \cos \pi/6) E_s}{2\alpha N_o}}\right) + \frac{1}{4} f\left(\sqrt{\frac{(\rho_1 - 1)^2 E_s}{N_o}}\right) \\ & + \frac{1}{8} f\left(\sqrt{\frac{1 E_s}{\alpha N_o}}\right) + \frac{3}{8} f\left(\sqrt{\frac{2\rho_2^2 \sin^2 \pi/12 E_s}{\alpha N_o}}\right) + \frac{1}{2} f\left(\sqrt{\frac{(\rho_2 - \rho_1)^2 E_s}{2\alpha N_o}}\right) \\ & + \frac{5}{8} f\left(\sqrt{\frac{2\rho_2^2 \sin^2 \pi/20 E_s}{\alpha N_o}}\right) + \frac{3}{4} f\left(\sqrt{\frac{(\rho_3 - \rho_2)^2 E_s}{2\alpha N_o}}\right) \\ & + \frac{7}{8} f\left(\sqrt{\frac{2\rho_3^2 \sin^2 \pi/28 E_s}{\alpha N_o}}\right) \end{aligned} \quad (14)$$

From the above inequality, we can be seen that all parameter values are known, and the SER upper bound of 64APSK can be obtained. By multiplying $h_{ij} \cdot \log_2^M$ the right items of the inequality, the upper bound of SER can be transformed into the expression of the upper bound of bit error ratio (BER). Where $h_{ij}$ is the Hamming distance between symbols $s_i$ and $s_j$ on the constellation. Specifically, if 64APSK adopts the constellation recommended in CCSDS131.2 blue book, its BER upper bound only needs to be obtained by multiplying the right side of the above formula by  $h_{1,2}=1/6, h_{1,3}= 2/6, h_{1,15}=1/6, h_{3,2}=1/6, h_{3,7}= 2/6, h_{7,6}=1/6, h_{7,13}= 2/6, h_{13,12}= 1/6$ .

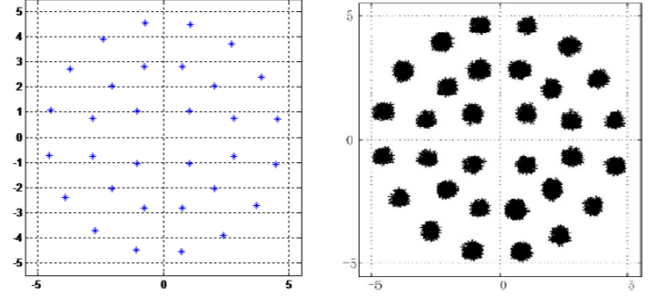


Figure 3: Constellation of 32APSK Transmitter and Receiver.

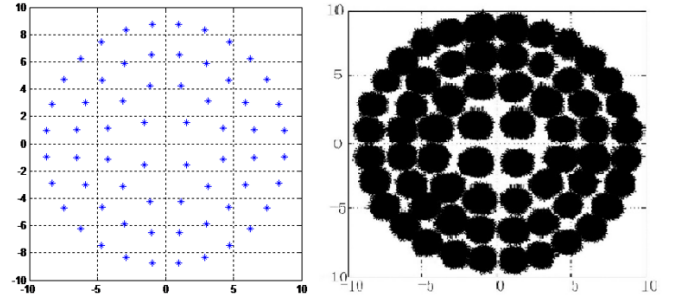
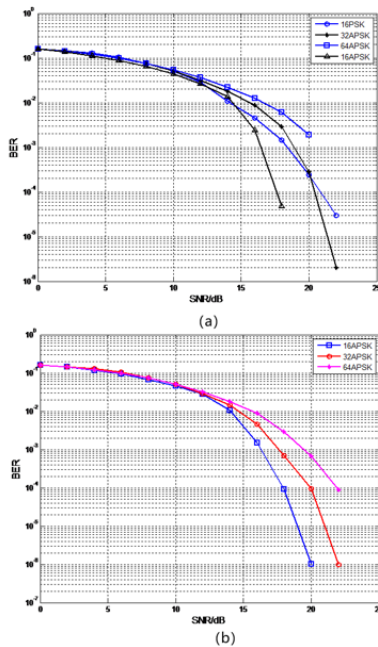


Figure 4: Constellation of 64APSK Transmitter and Receiver.

## 5 ALGORITHM PERFORMANCE SIMULATION VERIFICATION

The constellation diagrams of the transmitter and receiver of 32APSK and 64APSK are shown in Figure 3 and Figure 4. Obviously, the modulation process of 32APSK and 64APSK is dominated by phase modulation and supplemented by amplitude modulation. It can be seen from the transmitting constellation that the distribution density of star points is dense and uniform, and there is almost no space waste. It can be found from the receiving constellations that although they are high-order APSK modulation constellations, after 20dB and 25dB Gaussian channels, the boundary between all star points in 32APSK and 64APSK constellations is relatively clear, which can provide better demodulation conditions for later demodulation technology.

From the constellation diagram, compared with APSK demodulation mode, PSK mode distributes all star points on one circle, while APSK mode distributes all star points on multiple concentric circles with different radii. At the same modulation order, the density between star points of the former is significantly greater than that of the latter, so that the demodulation resolution decisions of the two at the receiver are completely different. Although the signal-to-noise ratio of modulation symbols with the same order is the same, the resolution limit between the receiving stars of the former is obviously blurred than that of the latter. The higher the order, the higher the degree of ambiguity, which will make the PSK



**Figure 5: Comparison of Bit Error Rate Performance of 16PSK, 16APSK, 32APSK and 64APSK.**

demodulation decision technology more difficult in the later stage of the system.

In the modeling conditions, it can be seen from Figure 5(a) that the BER of 16PSK after system demodulation decision is significantly higher than that of 16APSK. Especially, when the signal-to-noise ratio is 20dB, the performance of 32APSK is better than that of 16PSK. In addition, the bit error rate curve interval of 16PSK and 32APSK is significantly greater increasing, and the interval gap is twice. The steepness of the bit error rate curve of 32APSK is also significantly higher than that of 16PSK, indicating that with the increase of modulation order, high-order APSK still has a large technical application space, which is also an important reason for the possible use of high-order APSK in 6G oriented satellite communication.

The simulation BER curves of 16APSK, 32APSK and 64APSK simulated by soft demodulation are shown in Figure 5(b), and obvious demodulation results can be obtained. Soft demodulation refers to the method that the system demodulates information bits directly. When the modulation order is high, because the system needs to judge each bit in each symbol, the algorithm is much more complex than hard demodulation, but because it demodulates bits, the demodulation performance is also the best. Therefore, the performance of MAPSK in soft demodulation mode is better than that in hard demodulation mode, which can obtain better demodulation performance. It is a good high flux modulation and demodulation method.

## 6 CONCLUSION

With the integration of satellite communication system and 6G mobile communication system, this method makes full use of the

space in the constellation, makes the star points of high-order APSK reasonably and evenly distributed, increases the distance between adjacent star points, improves the resolution of the receiver constellation, and reduces the technical requirements of symbol decision at the receiver. It can be predicted that the existing communication system pattern and technology will change. Not only the most basic broadband communication technology will be introduced, but also MAPSK system will be used as much as possible in baseband modulation and demodulation technology.

## ACKNOWLEDGMENTS

I would like to express my sincere thanks to Mr. Yong Peng and other teachers at the same time. And the paper was supported in part by the National Nature Science Fund of China (NSFC)(No.61871471).

## REFERENCES

- [1] M.Q.Wu,W. Wu W, B.Zhou, *et al.* (2016). The architecture of the integrated space-terrestrial information network. *Satellite and Network*, 3: 30-36.
- [2] N. Zhang, K. Zhao, G. Liu (2015). Thought on constructing the integrated space-terrestrial information network. *Journal of China Academy of Electronics and Information Technology*, vol.10(3):223-230.
- [3] W. Saad, M.Bennis, Mingzhe Chen (2020). A vision of 6G wireless system :applications, trends, technologies, and open research problems. *IEEE Network*, vol.34(3):134-142.
- [4] Shafi, AF Molisch, M Dohler (2021). 6G wireless system: vision, requirements, challenges, insights, and opportunities. *Proceedings of the IEEE*, vol. 109(7):1166-1199.
- [5] Ms. Anju Uttam Gawas (2015). An overview on evolution of mobile wireless communication networks: 1G-6G. *International journal on recent and innovation trends in computing and communication*, vol. 34(3): 3130-3133.
- [6] Digital Video Broadcasting (DVB). Second generation framing structure,channel coding and modulation systems for broadcasting, interactive services, news gathering and other broadband satellite applications;part 1: DVB-S2. ETSI EN 302 307-1 V1.4.1, 2014.